

COMPARATIVE STUDY OF CORRELATION-BASED PIV EVALUATION METHODS*

R. Fei, L. Gui, W. Merzkirch

Lehrstuhl für Strömungslehre, Universität Essen, D-45117 Essen, Germany

Abstract. Several correlation-based PIV evaluation methods are compared by applying them to the evaluation of simulated PIV recordings, in which the particle images are distributed stochastically and have a Gaussian gray value distribution. The influence of particle image displacement and the influence of interrogation window size on the evaluation accuracy in uniform and in non-uniform flow were investigated. In all these cases the best results in terms of a statistical error are obtained with the MQD method.

Key words: PIV evaluation algorithm, cross-correlation.

1. Introduction

Many evaluation methods applied to planar PIV data sets are based on correlation schemes. Optical correlation resulting in visible patterns of Young's interference fringes has been abandoned in favour of digital image processing methods. The correlation algorithms reported by Cenedese and Paglialunga (1990), Adrian (1991), Willert and Gharib (1991) can be accelerated by the FFT. Another means of acceleration is the "error correlation" (Hart 1996). The correlation function also serves for evaluating the planar data field if the velocimetry is performed by particle tracking (Huang et al. 1993; Kemmerich and Rath 1994; Okamoto et al. 1995). The evaluation methods reported by Gui and Merzkirch (1996,1997) for tracking ensembles of particle images ("minimum quadratic difference" (MQD), "minimum absolute difference" (MAD) method) also incorporate the correlation function. The following algorithms that are described in the given references are investigated regarding their performance when certain parameters of the data sets and the evaluation procedure are varied.

2. Evaluation methods

2.1. Correlation A

This method, called Correlation A, is today widely used for the evaluation of PIV recordings. Its evaluation function is given this way:

$$\phi_A(m, n) = \sum_{i=0}^{M-1} \sum_{j=0}^{N-1} g_1(i, j) \cdot g_2(i + m, j + n) \quad (1)$$

*This research is supported by Deutscher Akademischer Austauschdienst (DAAD) with a grant for R. Fei.

Here, g_1, g_2 are the gray values in the interrogation window of size $M \times N$ pixel. In order to apply the FFT for acceleration, g_1, g_2 are assumed in this method as periodical functions with the periodicity M, N .

2.2. Correlation B

For the evaluation according to correlation B, g_1, g_2 should not be assumed to be periodical functions. The evaluation function is defined as:

$$\phi_B(m, n) = \frac{1}{(M-m) \cdot (N-n)} \sum_{i=0}^{M-m-1} \sum_{j=0}^{N-n-1} [g_1(i, j) - \bar{g}_1] \cdot [g_2(i+m, j+n) - \bar{g}_2] \quad (2)$$

for $m \geq 0, n \geq 0$.

Here \bar{g}_1, \bar{g}_2 are the average gray values in the interrogation window of the respective PIV recordings. The denominator $(M-m) \cdot (N-n)$ applies to the overlapping area of the interrogation windows to be correlated. If g_1, g_2 are no periodical functions, $g_2(i+m, j+n)$ has no value outside the interrogation window, if m, n are not zero. One way to overcome this problem is not to calculate the evaluation function outside the interrogation window. The calculation of the evaluation function will be carried out only in the overlapping area of the interrogation windows. (Cenedese and Paglialunga 1990; Okamoto et al. 1995).

2.3. Correlation C

$$\phi_C(m, n) = \sum_{i=0}^{M-m-1} \sum_{j=0}^{N-n-1} [g_1(i, j) - \bar{g}_1] \cdot [g_2(i+m, j+n) - \bar{g}_2]. \quad (3)$$

Like with "Correlation B", the calculation of the evaluation function according to "Correlation C" is carried out only in the overlapping area of the interrogation windows, but without dividing by the overlapping area of the interrogation window. (Cenedese and Paglialunga 1990; Okamoto et al. 1995).

2.4. Error correlation

It is common to accelerate the evaluation by applying the FFT. One of the alternative methods for increasing the speed of evaluation was reported by Hart (1996) and is named "error correlation".

$$\phi_E(m, n) = 1 - \frac{1}{(M-m)(N-n)} \sum_{i=0}^{M-m-1} \sum_{j=0}^{N-n-1} |g_1(i, j) - g_2(i+m, j+n)| \quad (4)$$

for $m \geq 0, n \geq 0$.

The time-consuming multiplication in the evaluation function Φ_E are avoided in this method. The evaluation is carried out only with additions and subtractions.

2.5. Correlation-tracking

$$\phi_T(m, n) = \sum_{i=0}^{M-1} \sum_{j=0}^{N-1} [g_1(i, j) - \bar{g}_1] \cdot [g_2(i + m, j + n) - \bar{g}_2]. \quad (5)$$

In correlation tracking this form of the correlation function is used as a tracking criterion for determining the displacement of a digital particle image pattern. g_1, g_2 should not be assumed to be periodical functions, and g_2 is no longer restricted to the interrogation window, $M \times N$ pixel, as in the correlation method, but it applies to a larger area, $(M + 2\rho) \times (N + 2\rho)$ pixel, of the PIV recording, see fig. 1. ρ is here the tracking radius which determines the maximal component of the particle image displacement that can be estimated by the tracking algorithm. (Huang et al. 1993; Kemmerich and Rath 1994; Okamoto et al. 1995).

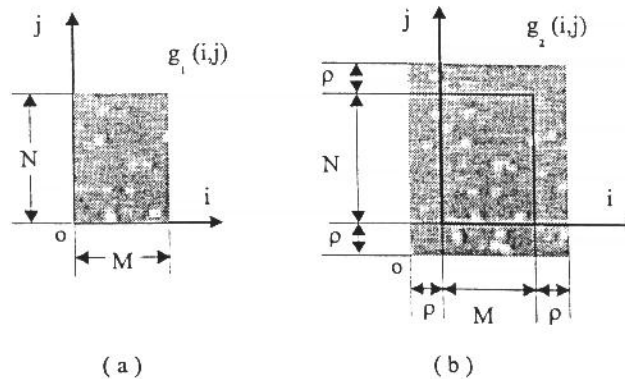


Fig. 1. The displacement of a digital particle image pattern.

2.6. MQD-tracking

For the MQD tracking method of Gui and Merzkirch (1996), the quadratic difference of the gray value distributions in the interrogation areas of the respective recordings is used as the evaluation function.

$$D_Q(m, n) = \sum_{i=0}^{M-1} \sum_{j=0}^{N-1} [g_1(i, j) - g_2(i + m, j + n)]^2. \quad (6)$$

The mean displacement of the particle images in the pattern is determined by the minimum of the difference of the gray value distributions.

2.7. MAD-tracking

In comparison with the "MQD tracking method", the MAD tracking method uses the absolute difference of the gray value distributions in the interrogation areas of the respective recordings.

$$D_A(m, n) = \sum_{i=0}^{M-1} \sum_{j=0}^{N-1} |g_1(i, j) - g_2(i + m, j + n)|. \quad (7)$$

3. Comparison of evaluation accuracy

The algorithms are compared by applying them to the evaluation of simulated (synthetic) PIV recordings, in which the position, size and brightness of the particle images are determined with random number distributions. The synthetic particle images are assumed to have a gaussian (exponential) gray value distribution. We get a pair of two identical particle image distributions by displacing the whole pattern of the first synthetic image with a known and constant displacement. The influence of three different parameters on the evaluation accuracy is studied.

3.1. Particle displacement

60 simulated pairs of PIV recordings of size 768×512 pixels and particle displacements ranging from 0.05 to 5 pixels are generated. The image density is 10 particle images in a 32×32 pixel interrogation window, and the particle image diameter is between 2 and 5 pixels. The gray value of the particle images is between 125 and 250. An example is given in fig. 2.

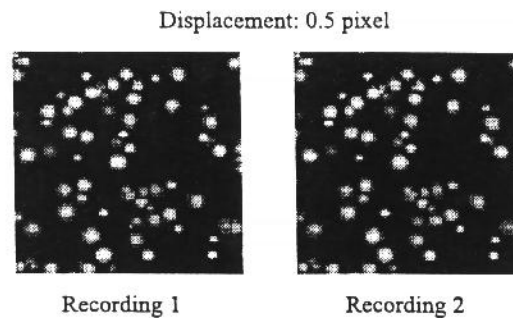


Fig. 2. Simulated recordings for uniform flow.

The RMS values of the evaluation errors, with reference to the known true displacement, are shown in fig. 3 for the different algorithms used. The errors determined for the

tracking algorithms are periodical functions with the periodicity of 1 pixel. The MQD method here produces the smallest error. The pattern shown for the correlation algorithms A,B,C can be improved by applying the window off-set technique (Westerweel et al. 1997), so that the displacement to be measured is reduced to values below 1 pixel.

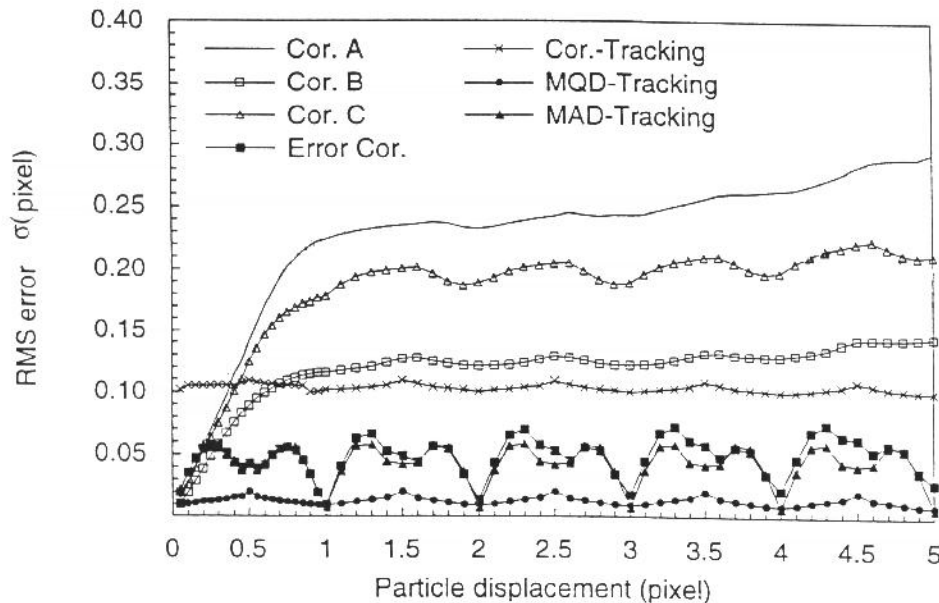


Fig. 3. Evaluation accuracy as function of particle displacement.

3.2. Interrogation window size

For investigating the influence of the interrogation window size on the evaluation accuracy, we choose a particle image displacement of 0.3 pixel for the simulated PIV recordings. 15 window sizes ranging from 16×16 to 128×128 pixels are used for the evaluation. The image density is 10 particle images in a 32×32 pixel interrogation window, and the particle image diameter is between 2 and 5 pixel. The gray value of the particle images is between 125 and 250. The resulting RMS errors are shown in fig. 4. The tendency is similar for all algorithms tested. The RMS error is large for the small window size and decreases rapidly with increasing window size. There are no large differences between the RMS errors for correlation A and C. The RMS errors for the error correlation method is nearly the same as that for the MAD tracking method. The influence of the window size is prominent for small windows. Low RMS error values for

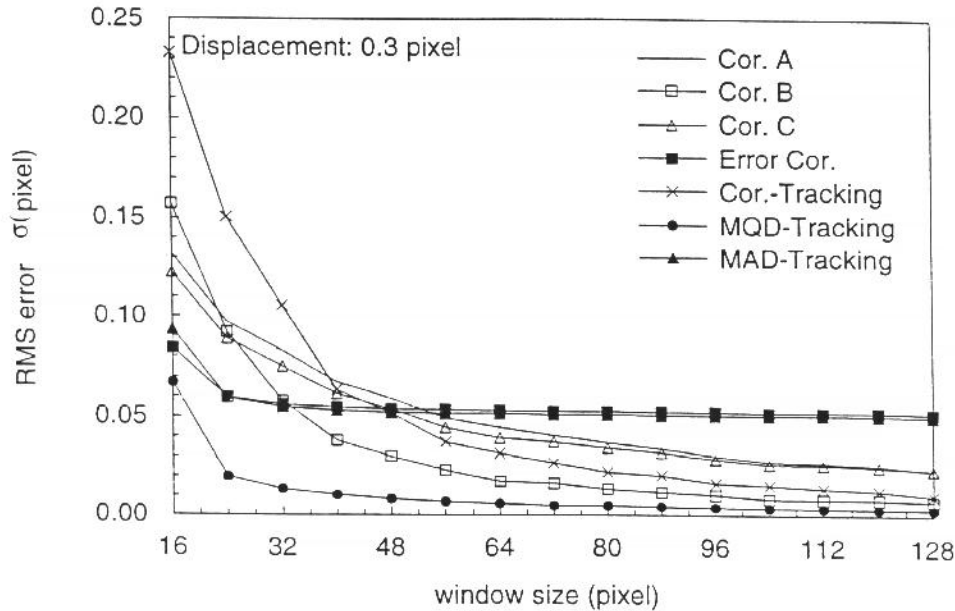


Fig. 4. Evaluation accuracy as function of interrogation window size in uniform flow.

small window sizes are mandatory for resolving small scale flow structures.

3.3. Non-uniform velocity fields

While the previous examples correspond to a constant velocity flow we use here the simulation of a PIV recording taken in a flow with strong non-uniformities (vortical flow). A synthetic PIV recording pair is generated with an average image density of 15 particle images in a 32×32 pixel interrogation window, and the other parameters, except for the particle image displacement, are the same as that described above. The known image displacement in this recording pair varies between 0 and 3 pixel, and its components S_x, S_y are determined by cosine functions as follows:

$$S_x = 3 \cos\left(\frac{x}{512}\right) \quad 0 \leq x \leq 768,$$

$$S_y = 3 \cos\left(\frac{y}{512}\right) \quad 0 \leq y \leq 512.$$

An example is shown in fig. 5. 15 window sizes ranging from 16×16 to 128×128 are used for the evaluation. The influence of the interrogation window size on the evaluation accuracy is tested; the RMS error shown in fig. 6 is the average error for the whole field

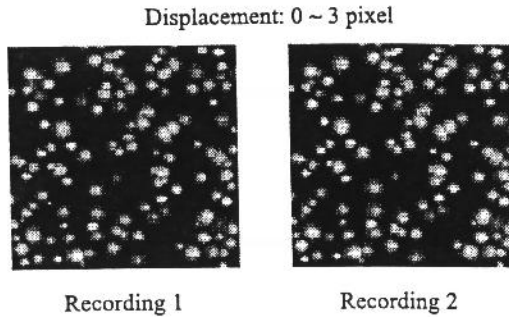


Fig. 5. Simulated recordings for non-uniform flow.

evaluated. In comparison to the pattern shown for the uniform flow, the RMS errors have here a different tendency. With increasing window size, the RMS error decreases first, then increases again. Each algorithm has a critical value for which the RMS error is minimal. The increase of the RMS error for increasing window sizes beyond the

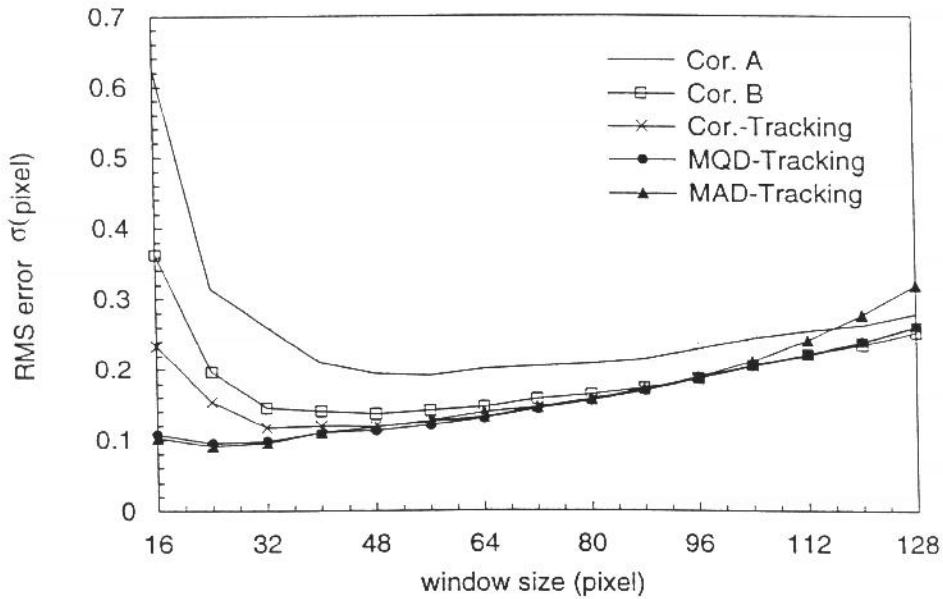


Fig. 6. Evaluation accuracy as function of interrogation window size in non-uniform flow.

minimum must be explained with the increasing non-uniformity of the particle image displacements included in the windows of larger size. The larger the window size, the stronger the non-uniformity, the larger the RMS error.

These parametric studies allow to select the appropriate evaluation algorithm if a specific accuracy is desired or needed. Additional parameters that are also investigated and of practical interest are the influence of particle image size and evaluation speed.

References

- 1990
- [1] Cenedese A., Paglialunga A. : Digital direct analysis for a multiexposed photograph in PIV. *Exp. Fluids* 8, 273-280.
- 1991
- [2] Adrian R.J. : Particle-imaging techniques for experimental fluid mechanics. *Annu.Rev.Fluid Mech.*, 23, 261-304.
- [3] Willert C.E., Gharib M. : Digital particle image velocimetry. *Exp. Fluids*, 10, 181-193.
- 1993
- [4] Huang H.T., Fiedler H.E., Wang J.J. : Limitation and improvement of PIV. Part I: Limitation of conventional techniques due to deformation of particle image patterns. *Exp. Fluids*, 15, 168-174.
- 1994
- [5] Kemmerich T., Rath H.J. : Multi-level convolution filtering technique for digital laser-speckle-velocimetry. *Exp. Fluids*, 17, 315-322.
- 1995
- [6] Okamoto K., Hassan Y.A., Schmidl W.D. : New tracking algorithm for particle image velocimetry. *Exp. Fluids*, 19, 342-347.
- 1996
- [7] Gui L., Merzkirch W. : A method of tracking ensembles of particle images. *Exp. Fluids*, 21, 465-468.
- [8] Hart D.P. : Sparse array image correlation. 8th Int. Sym. on Applications of Laser Techniques to Fluid Mechanics, July 8-11, Lisbon, Portugal.
- 1997
- [9] Gui L., Merzkirch W. : A fast mask technique for the phase-separated evaluation of two phase PIV recordings. 7th Int. Conf. on "Laser Anemometry Advances and Applications", September 8-11, Karlsruhe.
- [10] Westerweel J., Dabiri D., Gharib M. : The effect of a discrete window offset on the accuracy of cross-correlation analysis of digital PIV recordings. *Exp. Fluids* 23, 20-28.